Accepted Manuscript

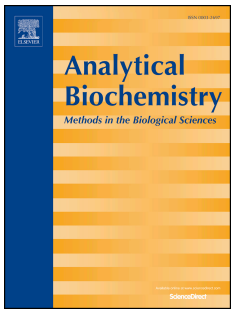

A high-throughput pH-based colorimetric assay: Application focus on alpha/beta hydrolases

Mariétou F. Paye, Harrison B. Rose, John M. Robbins, Diana A. Yunda, Seonggeon Cho, Andreas S. Bommarius

PII: S0003-2697(18)30265-3

DOI: 10.1016/j.ab.2018.03.009

Reference: YABIO 12962

To appear in: *Analytical Biochemistry*

Received Date: 30 November 2017

Revised Date: 26 February 2018

Accepted Date: 12 March 2018

Please cite this article as: Marié.F. Paye, H.B. Rose, J.M. Robbins, D.A. Yunda, S. Cho, A.S. Bommarius, A high-throughput pH-based colorimetric assay: Application focus on alpha/beta hydrolases, *Analytical Biochemistry* (2018), doi: 10.1016/j.ab.2018.03.009.

Manuscript Submission to Analytical Biochemistry
Subject Category: Enzymatic Assays and Analysis

A high-throughput pH-based colorimetric assay: application focus on alpha/beta hydrolases

Author Names and Affiliations

Mariétou F. Paye [1, ‡], Harrison B. Rose [2, ‡], John M. Robbins [2], Diana A. Yunda [1, 3], Seonggeon Cho [3], and Andreas S. Bommarius [1, 2, *]

[1] School of Chemistry & Biochemistry, [2] School of Chemical & Biomolecular Engineering, [3] School of Biomedical Engineering. Krone Engineered Biosystems Building, Georgia Institute of Technology, Atlanta, Georgia,30332, United States.

[‡] These authors contributed equally to this work. [*] Corresponding Author: Prof. Andreas Bommarius, 5018 Krone Engineered Biosystems Building, Georgia Institute of Technology, 30332-2000. Email: andreas.bommarius@chbe.gatech.edu

Abstract

Research involving α/β hydrolases, including α-amino acid ester hydrolase and cocaine esterase, has been limited by the lack of an online high throughput screening assay. The development of a high throughput screening assay capable of detecting α/β hydrolase activity toward specific substrates and/or chemical reactions (e.g., hydrolysis in lieu of amidase activity and/or synthesis instead of thioesterase activity) is of interest in a broad set of scientific questions and applications. Here we present a general framework for pH-based colorimetric assays, as well as the mathematical considerations necessary to estimate *de novo* the experimental response required to assign a 'hit' or a 'miss,' in the absence of experimental standard curves. This combination is valuable for screening the hydrolysis and synthesis activity of α/β hydrolases on a variety of substrates, and produces data comparable the current standard technique involving High Performance Liquid Chromatography (HPLC). In contrast to HPLC, this assay enables improved efficiency obtained from a single experiment.

1 Introduction

1.1 AEH and CocE Enzymes

Hydrolases are ubiquitous enzymes involved in a myriad of chemical processes and are essential to the survival of all living organisms.[1] The most widely studied enzymes in this class are in the α/β hydrolase family, which have applications in analytical, industrial, and pharmaceutical fields. Some uses include synthesis of β-lactam antibiotics (β-LA) with α amino acid ester hydrolase (AEH, Figure 1 A),[2] treatment of cocaine addiction with cocaine esterase (CocE, Figure 1 B),[3] and hydrolysis of insecticides by organophosphorus hydrolase (reaction scheme not shown).[4]

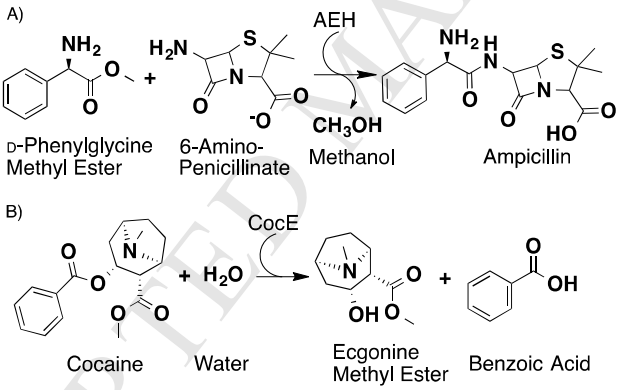

Figure 1: Popular applications of the α-amino acid ester hydrolase (AEH) and cocaine esterase (CocE) enzymes used in this study. A) AEH catalyzes the synthesis of ampicillin from D-phenylgylycine methyl ester and 6-aminopenicillinate B) CocE catalyzes the hydrolysis of cocaine into benzoic acid and ecgonine methyl ester.

There have been intensive efforts to identify amino acid substitutions and reaction conditions that improve thermostability and catalytic rates of AEH and CocE. [3, 5] However, those efforts have been limited by dependence on HPLC-based assays, which are low throughput and resource-intensive. Thus, an alternative, high-throughput assay is desirable to accelerate the process of generating improved enzyme variants. For this purpose, a model reaction in which AEH or CocE catalyzes the sequential peptide synthesis of multiple D-phenyl glycine methyl ester (D-PGME) molecules, thus resulting in a mixture of various peptide methyl esters, has been proposed (Figure 2).[6] A crucial side-reaction also catalyzed by these enzymes is the primary hydrolysis of D-PGME, which releases D-phenyl glycine (D-PG) and methanol (Figure 2). Because hydrolysis of the reacting methyl ester limits the amount of active substrate available for the synthesis reaction, biocatalysts capable of promoting the synthesis reaction while suppressing, if not blocking completely, the hydrolysis reaction is coveted by industry.[7] Given the need for a less resource-intensive analytical method, the current study serves to utilize this model reaction to identify a high throughput assay capable of differentiating between the ester hydrolysis and amide synthesis reactions in general.

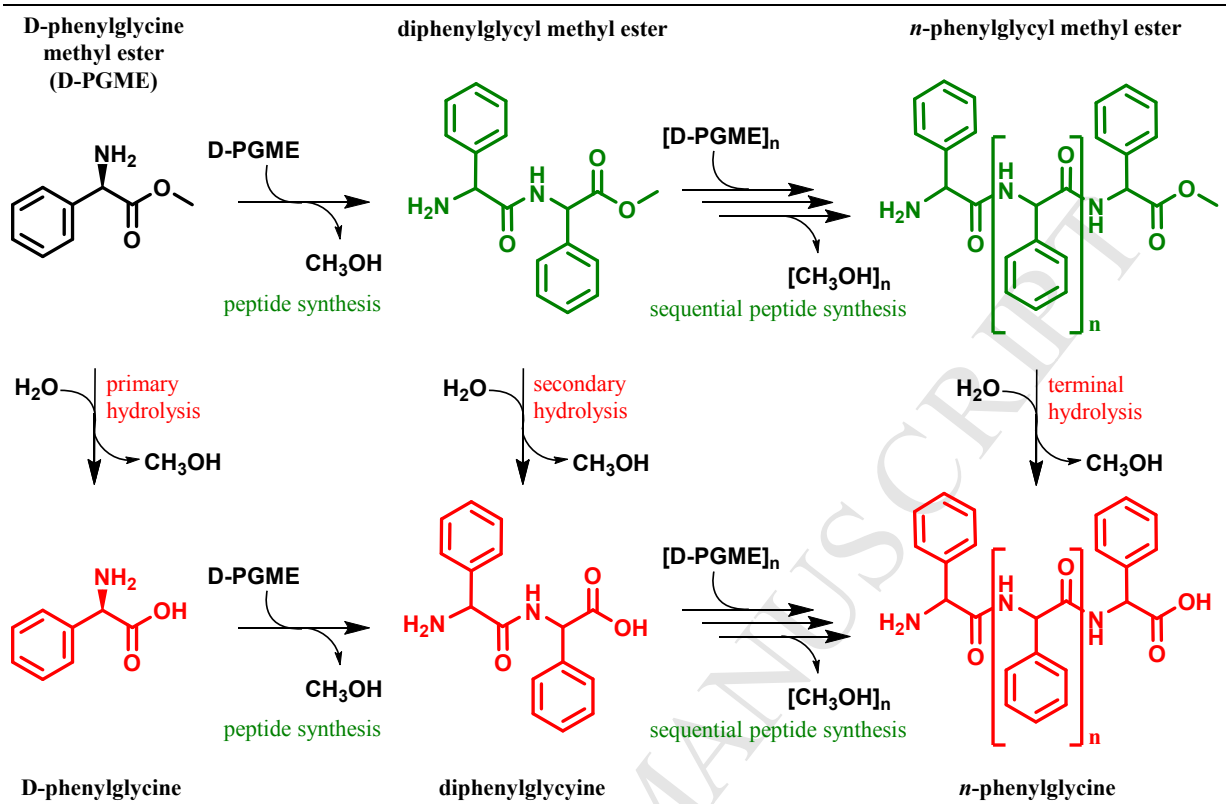

Figure 2: Proposed scheme for the α-amino ester hydrolase (AEH) or cocaine esterase (CocE) catalyzed model reaction of D-PGME to various products. Sequential peptide synthesis reactions (left to right) are proposed to occur in competition with ester hydrolysis reactions (top to bottom).

1.2 Literature Survey of Existing Assays

Since the substrates and products (i.e. primary amines and carboxylic acids, respectively) of these enzymes have labile protons, it was proposed that weakly buffered systems may experience a change in pH value over the course of ester hydrolysis or amide synthesis reactions such as those shown in Figure 1 and Figure 2. The use of pH-based colorimetry to detect enzyme activity has been reported with certain hydrolases (enantioselective hydrolases),[8] transketolases (e.g., TK, EC 2.2.1.1),[9] transferases (e.g., galactosyltransferase),[10] acylases (e.g. cephalosporin C acylase),[11] and kinases (e.g., glucokinase).[12] These published assays are dependent on low buffering capacity and salt content, selection of pH-indicator based on initial pH (the pK_a of the indicator should equal the starting pH), and high concentrations of pH-indicators. Additionally, each set of conditions requires unique standard curves, which are time-consuming to collect. Collectively, these restrictions limit the extent to which various substrates and reaction conditions can be explored, and the rapidity with which such investigations can be conducted.

Two colorimetric assays for AEH activity have been described previously, one endpoint assay, and one for real-time monitoring (see Figure S-2 in the Supporting Information). The endpoint assay is designed to measure the absorbance of the chromophore diketopiperazine (DKP) derivative, which is formed by ring-opening of β-LA coupled with nucleophilic attack by reduced ascorbic acid[13] However, the reaction does not effectively distinguish between substrates and products.[14] On the other hand, the real-time assay tracks the production of the chromophore 5-amino-2-nitrobenzoic acid, which is produced by hydrolysis of an AEH substrate analog, 5-(2'-amino-5-phenylacetamido)-2-nitrobenzoic acid (APANiB).[14] APANiB is not commercially available and is difficult to synthesize due to its precursors' tendency to self-polymerize.

Similarly, a real-time CocE assay using substrate analogs has been reported.[15] In this assay scheme (illustrated in Figure S-2 of the Supporting Information), enzymatic cleavage of the thioester bond in benzoyl-3-mercapto ecgonine methyl ester produces benzoate and 3-mercapto ecgonine methyl ester, which is reacted with 5-5'dithiobis(2-nitrobenzoic acid) (DTNB, Ellman's reagent) to produce 3-5' dithio(ecgonine methyl ester)- (2-nitrobenzoic acid), and the chromophore, 5-mercapto-2-nitrobenzoic acid.[15] However, this assay is limited to detecting thioesterase activity and requires the use of a thioester analog of each target substrate.

1.3 Generalizing pH-based Colorimetric Assays

The development of an improved assay method was motivated by the challenges surrounding current AEH and CocE assays, as well as pH-based assays in general. In reaction theory, conversion is a single value that encapsulates the multitude of variables related to the progress of a reaction or, in an assay context, the success of a catalyst. We present a general mathematical approach for creating a direct mapping between the absorbance of a colorimetric indicator and the conversion of a pH-altering reaction. Our model quantitatively predicts how an assay will respond to a reaction, eliminating the need for experimental standard curves in 'hit' or 'miss' activity assessment and reducing the time and material resources needed to conduct high throughput screens, and even enabling real-time monitoring and hypothesis testing. Assay response curves are typically unintuitive – changes in solution pH tend to be accompanied by changes to ionic strength which in turn alter the effective pK_a values of participating species and may broaden, narrow, or shift the buffering capacity of the reaction mixture. By allowing operators to visualize the response and sensitivity of an assay to each design parameter, these tools can also serve to support and inform decisions made in assay development and troubleshooting. We present some examples of general experimental guidelines and troubleshooting recommendations that have been borne out by the modeling in this manner.

For aqueous hydrolysis reactions of known stoichiometry, it is possible to estimate the degree of conversion that is required to produce a particular pH value, so long as the starting concentrations and acidity constants of all species are known. Generally, pH can also be related to the color of a halochromic indicator. Phenol red was selected as the indicator for this work, as it exhibits a visible color change over the pH range (4.5-8.5) of interest for monitoring hydrolysis and synthesis reactions. By combining these relationships, it is possible to predict the spectrophotometric response of a hydrolysis reaction. Plots of absorbance vs. hydrolysis conversion produced with this method can be used to identify assay conditions that provide reasonable sensitivity and to rule out specific reactions for which pH-based assays are inappropriate. Once experimental absorption data (either endpoint or real-time) are collected, the predicted responses may be used in lieu of experimental standard curves for data interpretation and rapid qualification of "hits" and "misses."

In the sections that follow, we validate and demonstrate this approach to pH-based colorimetric assays in several steps. First, we compare enzymatic reaction data obtained by high performance liquid chromatography (HPLC) using *traditional* standard curves (i.e., for quantification of individual species) with data obtained by colorimetry using *simulated* standard curves (i.e. solutions that have been deliberately prepared to simulate the state of a reaction system at a given level of conversion). Next, we compare *predicted* standard curves (i.e., calculated by the model without fitting) to those *simulated* standard curves. Finally, we use the *predicted* standard curves from the model to interpret experimental enzymatic reaction data and perform hypothesis testing to demonstrate "hit" or "miss" screening. The proposed workflow for an assay experiment with hypothesis testing is illustrated in Figure 3 (and in more detail in Figure S-1 of the Supporting Information).

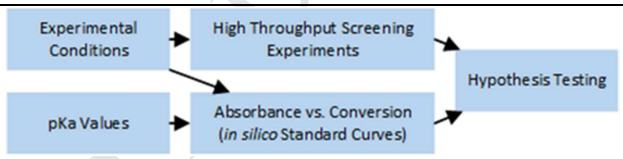

Figure 3: The workflow required to use the generalizable pH-based colorimetric assay. The experimental conditions used in wet lab experimentation are tabulated and combined with existing knowledge of substrate, product, and buffer pKa values, which are used to predict the relationship between spectrophotometric measurements and reaction conversion. Experimental data and predicted relationships are then combined to perform hypothesis testing and qualify each experiment as either a hit or a miss.

2 Materials & Methods

2.1 Materials

Sodium dodecyl sulfate, nicotinamide, D-phenylglycine methyl ester, phenol red, and methyl picolinate were purchased from Sigma Aldrich while acetamide, nicotinic acid, imidazole, and picolinic acid were purchased from Alpha Aesar. Other commercial sources include Fisher Scientific for ammonium acetate, sodium hydroxide, and HPLC-grade acetonitrile; Fluka Chemika for 6-aminopenicillanic acid and D-phenylglycine; VWR analytical for dibasic anhydrous sodium phosphate and sodium chloride. Other purchased materials were sodium ampicillin (Gold Biotechnology), Overnight Express (Novagen), monobasic sodium phosphate monohydrate (J.T. Baker), molecular biology grade LB broth lennox (US Biological Life Sciences) and hydrochloric acid (Acros Organics). The expression vector for α-amino acid ester hydrolase (AEH) was produced by a past member of this research group[6, 16] while that for cocaine esterase was graciously donated by Dr. Neil Bruce's laboratory at the University of York, UK.

2.2 Protein Expression and Purification

Both AEH and CocE were expressed in Rosetta™(DE3)pLysS competent cells (Novagen) using pET28 and p234 under selective pressure from kanamycin and ampicillin-carbenicillin, respectively. Because wildtype AEH is not thermostable, only its quadruple variants H (N186D/A275P/V622I/E143H: AEH QV-H) and G (N186D/A275P/V622I/E143G: AEH QV-G) were used in this paper.[16] Chloramphenicol was used to maintain the plasmid supplying tRNAs for exogenous codons. 5 mL seed cultures (LB broth, 37 °C, 200 rpm) were grown overnight, passaged to 200 mL of Overnight Express, and incubated for an additional 8 hours (37 °C, 250 rpm). Cultures were incubated at room temperature for 16 hours after which they were centrifuged. The resulting pellets were suspended in lysis buffer (18 mL per 1 g of pellet; 10 mM Imidazole, 50 mM $NaPO_4$, 300 mM NaCl, pH 8.0) and lysed by sonication on ice. Enzymes were purified by nickel affinity chromatography with Novagen Ni-NTA HisBind Resin. Bound proteins were washed (1 mL of 50 mM Imidazole, 50 mM $NaPO_4$, 300 mM NaCl, pH 8.0; repeated 20x), followed by 1 mL washes with buffers containing imidazole increasing in concentration from 60 mM to 240 mM in 20 mM increments (remaining buffer composition: 50 mM $NaPO_4$, 300 mM NaCl, pH 8.0). Washed proteins were eluted with 8 mL of elution buffer (250 mM Imidazole, 50 mM $NaPO_4$, 300 mM NaCl, pH 8.0). For each enzyme, the combined fractions were dialyzed twice against 2 L of dialysis buffer (100 mM $NaPO_4$, 100 mM NaCl, pH 7.0) to remove the imidazole, which inhibits enzyme activity. Purified enzyme was quantified using Bradford reagent at the absorbance maxima of 595 nm.

2.3 Enzymatic Hydrolysis and Synthesis Reactions

Five types of hydrolysis and synthesis reactions were carried in this study: the reactions of (1) 6-aminopenicillinate and D-phenylglycine methyl ester to ampicillin and methanol; (2) methyl picolinate to picolinate and methanol; (3) ampicillin to 6-aminopenicillinate and D-phenylglycine; (4) D-phenylglycine methyl ester to D-phenylglycine and methanol, (5) and D-phenylglycine methyl ester to di- and tri-peptides and methanol.

All reactions were carried out in 96-well clear flat-bottom plates at room temperature in 200 μL of 100 mM sodium phosphate buffer with 20 μM phenol red. Substrates were added to the required concentration, which varied between experiments. Reaction start-time was taken upon addition of purified enzyme, either CocE or AEH. Enzymes were suspended in dialysis buffer and added to the required final concentration. Non-enzymatic controls were prepared using dialysis buffer without enzyme. Additional controls were performed to verify that phenol red is neither a substrate nor an inhibitor of CocE or AEH, including trials with enzyme and substrate but without phenol red, as well as with enzyme and phenol red in the absence of substrate. These controls are described in the Supporting Information, in the section titled *Validation of Phenol Red*.

Reactions were monitored with direct measurements of product formation by high performance liquid chromatography (HPLC) using a Shimadzu HPLC 20A (DGU-$20A_5$, LC-20AT, SIL-20AC HT, CBM-20A, SPD-M20A, CTO-20A) and a reverse-phase Phenomenex C-18 column (Luna 5 μ C18 (2) 100 Å 250×4.60 mm 5 micron). The mobile phase consisted of 70% 5 mM phosphate buffer at pH 3.0 with 300 mg/L SDS and 30% acetonitrile supplied at a rate of 1 mL/minute. Reaction time points were taken by 10-fold dilution of reaction aliquots into the mobile phase. Diluted samples were then supplied to the column in a 2.0 μL injection. Column eluent was monitored at 215 nm to monitor all substrates and products.

The pH of each reaction mixture is an aggregate result of the relative buffering capacity contributions of the background buffer, the reaction substrate(s) and the reaction product(s). For that reason, the pH value of each sample was indirectly monitored by tracking changes in the absorbance of phenol red on a Biotek Synergy H4 Hybrid (plate) reader. Absorbance measurements were taken over time at 557 nm and 479 nm, the alkaline absorbance maximum and isosbestic point of phenol red, respectively. All downstream data processing was performed using the (557 nm/479 nm) absorbance ratio. Full wavelength scans from 300 nm to 700 nm were also performed on each well after 4 hours to check for baseline deviation.

2.4 Simulated Conversion Standard Solutions

Samples were prepared to standardize the spectrophotometer analyses for each hydrolysis and synthesis reaction. Stock solutions of reactants were prepared in 100 mM sodium phosphate. For reasons discussed later in the modeling section, precise accounting of total ions is critical to the success of this method. The sodium concentration was adjusted to give the reactant stocks a pH value of 7.0. Individual product stocks were prepared in a 2x buffer of the same relative salt composition as the reactant stocks, such that mixing the reactant and corresponding product stocks in predefined ratios simulates a desired conversion without changing the buffer composition. For example, mixing a 1:3:3 ratio of the stocks for a reactant and both products generates a solution with the same composition and pH as a reaction at 75% conversion. Each sample was evaluated by spectrophotometry and HPLC as described above.

2.5 Determination of Enzymatic Kinetic Parameters

Using the simulated conversion standards to interpret the spectrophotometric and HPLC data, initial rates were determined in triplicate for each reaction in both the presence and absence of enzyme. The contribution of

chemical (non-enzymatic) hydrolysis was subtracted, and the kinetic parameters were determined from the best fit of data to the Michaelis-Menten equation using Kaleidagraph[1].

2.6 Characterization of Phenol Red

In addition to spectrophotometric evaluation of the simulated conversion standards, a 20 μM solution of phenol red in 100 mM phosphate buffer was titrated with sodium hydroxide (10 N) and hydrochloric acid (6 N) to reveal the dependence of its absorption spectrum on pH in the absence of other compounds.

2.7 Modeling and Prediction of Assay Response Curves

A general mathematical model was developed to predict how the colorimetric assay would respond to different hydrolysis reactions. The predictions are used for experimental planning, and to interpret experimental results for hypothesis testing, as described below.

Hydrolysis reactions examined here are of the general form $A + water \rightleftharpoons B + C$ where A, B, and C may be weakly acidic or basic. Model formulation begins with the general consideration of a weak acid reversibly dissociating in aqueous solution: $AH_j^{z+1} \rightleftharpoons H^+ + AH_{j-1}^{z}$ where z is the charge of the conjugate base and j is the number of labile protons in each protonation state.

The degree to which a weak acid dissociates is typically reported as a pK_a value which may be presented as a pK_a^c ('concentration basis'), pK_a^{th} ('thermodynamic value' or 'activity-basis'), or pK_a^* ('mixed-mode' or 'practical'), depending on the data source and application.[17] [2] pK_a values determined using a potentiometric pH probe are typically in the form of pK_a^*, unless they have been extrapolated to infinite dilution (pK_a^{th}), or the probe has been standardized using particularly rigorous methods (pK_a^c).[18] Acid-base equilibria inherently involve charged species and are sensitive to (and result in) changes in ionic strength. As a result, deviations between pK_a^c, pK_a^{th}, and pK_a^*, as well as between activity- and concentration-based measures of pH tend to increase with increasing ionic strength.

The concentration-based pK_a value, pK_a^c, may be written as the sum of the thermodynamic value and a 'lumped activity coefficient' correction factor that is dependent on ionic strength. To keep this model as general as possible, an extended Debye-Hückel relationship is used to estimate the correction factor. This correction can be expressed as a special case of the correlation derived by Sun et al:[19]

$$pK_a^c = pK_a^{\mathrm{th}} + (1.02z)\left(\frac{\sqrt{I}}{1+A\sqrt{I}} + BI\right) - CI \qquad (1)$$

where z is the charge of the conjugate base, I is the ionic strength, and $A, B,$ and C are empirically derived parameters with mean values of 1.50, -0.09, and -0.09, respectively. The correction is valid up to ionic strengths of $I = 0.5$ M, and enables the use of concentrations rather than activities elsewhere in this model. A detailed explanation of this correction is provided in the Supporting Information.

Similarly, pH can be adjusted for ionic strength, to convert between the concentration-based value, pH_c, and the activity-based value, pH_a, with the latter corresponding to readings from a typical potentiometric pH electrode.

$$pH_a = pH_c + 0.51\left(\frac{\sqrt{I}}{1+1.50\sqrt{I}} - 0.11I\right) \qquad (2)$$

where

$$pH_c = -\log_{10}([H^+]) \qquad (3)$$

Finally, these general relationships may be used to determine the distribution of protonation states:

$$pK_{a,i,j}^{\mathrm{c}} = -\log_{10}\left(\frac{[AH_{j-1}]\times 10^{-pH_c}}{[AH_j]}\right) \qquad (4)$$

for all ionizable species, i, and number of labile protons, j. Note that pH_c is used here to avoid over-correcting for ionic strength.

The protonation state of water can also be represented, using the definition of the ionic product of water:

$$[OH^-] \times 10^{-pK_W^c} = 10^{-pH_c} \qquad (5)$$

Here also, pH_c is used. The value of pK_W may be corrected as in Equation 1, however, a value of $z = 1$ must be used.

It is necessary to link these expressions together using a charge balance:

$$0 = \sum_i \sum_j \left(c_{i,j} \times z_{i,j}\right) \qquad (6)$$

where $c_{i,j}$ and $z_{i,j}$ are the molar concentration and charge number of each ion in each protonation state, respectively. If the solutions are titrated to a specific pH and/or prepared using salts, then the concentrations of the co-salt ions and titrants must be included in the charge balance equation. Precision is required in the accounting of all salt species. An error in accounting for a monovalent anion on paper, for example, is comparable to the erroneous addition of hydrochloric acid in the laboratory.

Additionally, since specific protonation states cannot be measured or pipetted, total concentrations are used to specify and track the analytical composition of the reaction system:

[1] Synergy Software, KaleidaGraph V4.1.1, Reading, PA (1986-2000)

[2] A complete discussion of these bases, with guidelines for standardizing literature values to a thermodynamic basis is provided in the Supporting Information. Additionally, a tool for standardizing and curating pK_a values is provided in the first 'sheet' of the spreadsheet accompanying this publication.

$$c_{i,tot} = \sum_j (c_{i,j}) \quad (7)$$

This treatment is not necessary for the concentrations of sodium and chloride, as both can be calculated based on solution and stock preparation, and are assumed to be fully dissociated.

To predict the spectrophotometric response of the system due to the colorimetric indicator, the ratio of the molar extinction coefficient at one select wavelength relative to that of the isosbestic point is calculated for each protonation state of the indicator:

$$Abs_j = \frac{Abs_{j,\lambda_{sensitive}}}{Abs_{\lambda_{isosbestic}}} \quad (8)$$

When phenol red is used as the assay indicator, we use 557nm for $\lambda_{sensitive}$ and 479 nm for $\lambda_{isosbestic}$.

Next, the sum of the absorbance ratios of all protonation states of the indicator is normalized by the total indicator concentration:

$$Abs = \frac{\sum_j (Abs_j \times c_{indicator,j})}{C_{indicator,tot}} \quad (9)$$

It is also necessary to define the stoichiometric relationships between the reacting species in a manner that considers the conversion of the enzymatic reaction, and accounts for the possibility of non-zero starting concentrations of the products:

$$\begin{aligned} [A_{tot}] &= [A_{init}] \times (1 - X) \\ [B_{tot}] &= [B_{init}] + [A_{init}] \times X \\ [C_{tot}] &= [C_{init}] + [A_{init}] \times X \end{aligned} \quad (10)$$

The inclusion of the reaction in this manner relies on the assumption that the acid-base equilibrium reactions are significantly faster than the enzymatic reaction for any level of reaction conversion.

The ionic strength of the solution is dependent on the distribution of charged species present, and is calculated as follows:

$$I = \frac{1}{2} \sum_i \sum_j (c_{i,j} \times z_{i,j}^2) \quad (11)$$

Relating the total absorbance of the reacting mixture to its conversion requires solving the system of Equations (1-11). These equations are written in their expanded forms with additional explanation in Table S-4 of the Supporting Information.

In general, models of this form can be difficult to solve numerically, as the species concentrations spanning several orders of magnitude makes them poorly scaled. It is also difficult to solve such systems analytically for pH as a function of the species distribution. As such, approximations and simplifying techniques are frequently deemed necessary to make even seemingly straightforward buffer calculations (such as those without ionic strength corrections or concurrent hydrolysis reactions) more mathematically tractable.[20]

However, by treating pH_c as the independent variable, it is possible to solve the system of Equations (3-11) algebraically. Solution sets are defined by fixed parameters, including the initial assay composition ($[A]_{init}$, $[B]_{init}$, $[C]_{init}$, $[Phos]_{tot}$, $[Indicator]_{tot}$, $[Na^+]$, and $[Cl^-]$), thermodynamic ionization constants $pK_{a,i,j}^{th}$, and indicator absorptivities Abs_j. Wolfram Mathematica[3] was used to solve Equations (3-11) symbolically, producing algebraic expressions for ionic strength, absorption, and conversion as functions of pH_c.[4] These expressions are embedded within a MATLAB[5] framework, which allows them to be easily evaluated for a variety of reactions and reaction conditions which are specified within an accompanying spreadsheet.

In each execution of the MATLAB code, the complete expression for ionic strength is evaluated over a range of pH_c values, using the thermodynamic values for each acid dissociation constant. The calculated ionic strengths are then used in Equation (1) to estimate the concentration-based pK_a^c value of each species over the pH_c range, and the ionic strength is calculated again, using the new pK_a^c values. Three such iterations are typically sufficient for reasonable convergence. The resulting pK_a^c values are then used in the evaluation of the complete expressions for absorbance and conversion at each pH_c value. Finally, pH_a is calculated as described in Equation (2), so that the pH axis of the displayed data plots will correspond to traditional potentiometric measurements. A guide to using the accompanying MATLAB script is provided in the section 'Modeling Quick-Start Guide' of the Supporting Information, and a more detailed explanation can be found in the section titled 'MATLAB Script Explanation.'

As it is unlikely that perfect information will be available when parameterizing the model, the model framework has been structured to draw parameters from distributions mimicking the uncertainty of the experimental information. When using this Monte Carlo approach, reasonable estimates of uncertainty in model parameters (standard deviations of ± 0.1 on pK_a^{th} values and $\pm 2.5\%$ on nonzero concentrations) are sufficient to encompass most of the experimental simulated conversion data. Implementation of Monte Carlo uncertainty propagation and sensitivity analysis in the model are discussed in more detail in the 'Model Resolution, Sensitivity, and Error Analysis' section of the Supporting Information.

[3] Wolfram Research, Inc., Mathematica, Version 10.4, Champaign, IL (2016)

[4] The Mathematica inputs and outputs are provided in the Supporting Information, in sections 'Mathematica Input: Solving the Model Equations' and 'Mathematica Output: Expressions for Absorbance, Conversion, and Ionic Strength' respectively, as well as in the accompanying Mathematica Notebook file.

[5] MATLAB Release 2016a, The MathWorks, Inc., Natick, MA.

This model was used to predict assay response curves that might be observed under various conditions for each of the hydrolysis reactions considered, as well as to estimate the uncertainties associated with each prediction. Each prediction was initialized using a spreadsheet containing the model parameters, including the initial experimental conditions of the assay reaction, as well as the charges and pK_a^{th} values of each of the ionizable species. An example spreadsheet for initializing the model is also included in the Supporting Information section titled 'Excel Spreadsheet.' The charges and ionization constants used in this study are listed in Table S-3 of the Supporting Information.

2.8 Hypothesis Testing

The predicted relationship between reaction conversion and absorbance ratio can be used to interpret experimentally measured absorbance ratios as reaction conversions, with appropriate levels of uncertainty. This calculation can be performed for both enzymatic and non-enzymatic experiments, and their interpreted conversion levels can then be compared to determine if the presence of an enzyme has any effect on reaction conversion. This comparison requires the formation of two hypotheses: H_0 (the null hypothesis), which states that the enzyme has no impact on reaction conversion (an assay 'miss'), and H_1 (the alternative hypothesis), which states that the enzyme does impact the reaction (an assay 'hit'). The 'Welch's t-test,' using the Welch-Satterthwaite equation to estimate the underlying degrees of freedom, is applied to determine the probability that the enzymatic and non-enzymatic conversion values are equal.[21] Finally, using any desired p-value threshold α, the null hypothesis H_0 is either accepted or rejected. This analysis can be performed with a single set of experimental measurements or with time-series kinetic data, and is performed automatically with the spreadsheet supplied in the Supporting Information.

3 Results

3.1 Characterization and Validation of Phenol Red

The color change of phenol red over a range of pH values from 6.2 to 8.1 is presented in Figure 4. Full absorption spectra of phenol red under varied conditions and over a broader range of pH values are provided in Figure S-4 of the Supporting Information. After baseline removal, spectrophotometric analyses of reactions were performed by normalizing (Figure S-5 in the Supporting Information) the absorbance at 557 nm by that at the isosbestic point, 479 nm, and nonlinear regression was performed in MATLAB (Figure S-6) to parameterize the model. No change in the absorbance of phenol red was detected in the presence or absence of CocE (Figure S-7 in the Supporting Information), and HPLC analysis of reaction controls revealed no change in the activities of either CocE or AEH in the presence or absence of phenol red (Figure S-8 in the Supporting Information). These results suggest that phenol red is neither a substrate nor an inhibitor of the enzymes used in this study.

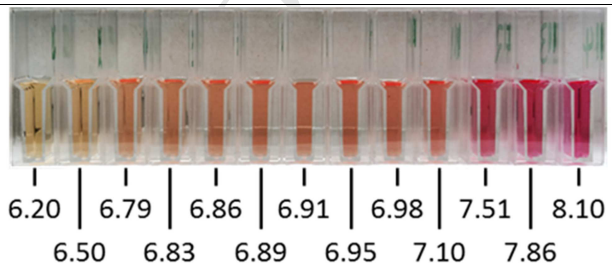

Figure 4: The color change of 20 μM phenol red in 100 mM sodium phosphate over a range of pH_a values from 6.20 to 8.10. This broad range of pH sensitivity makes phenol red a suitable indicator for assaying a wide variety of hydrolysis and synthesis reactions.

3.2 Evaluation of Hydrolysis Activity by Colorimetry and HPLC

To validate the colorimetric assay, both HPLC and spectrophotometry were used to evaluate enzymatic hydrolysis activity and the results were compared. Two reactions were tested: the hydrolysis of methyl picolinate by CocE (Figure 5), and the hydrolysis of ampicillin by AEH variant QV-G.

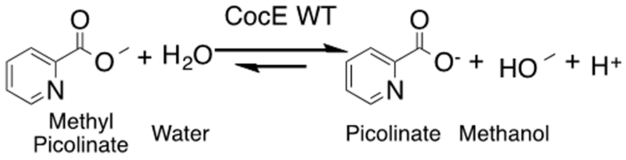

Figure 5: Cocaine Esterase (CocE) catalyzes the hydrolysis of methyl picolinate, producing picolinate and methanol. The carboxylic acid group on picolinic acid will release a proton under basic or neutral conditions, allowing the progress of this reaction to be tracked by indirect (spectrophotometric) monitoring of the solution pH using phenol red.

Experimental data and kinetic parameters for the hydrolysis of methyl picolinate by CocE are presented in Table 1, while experimental data and kinetic parameters for the hydrolysis of ampicillin by AEH variant QV-G are presented in Figure S-10 of the Supporting Information. Plots of CocE (0.148 μM) hydrolysis activity monitored by both colorimetric and HPLC methods as a function of methyl picolinate concentration are shown in Figure 6, and fitted kinetic parameters are reported in Table 1 (±SE). Parameter values determined by colorimetry ($K_M = 17.3 \pm 5.6$ mM, $V_{max} = 234 \pm 18$ pmole/s, $k_{cat} = 7.89 \pm 0.60\ M^{-1}s^{-1}$ [CocE] = 0.148 μM) were consistent with those determined by HPLC ($K_M = 14.02 \pm 6.7$ mM, $V_{max} = 196 \pm 20$ pmole/s, $k_{cat} = 6.62 \pm 0.70\ M^{-1}s^{-1}$, [CocE] = 0.148 μM). Additionally, values of V_{max} were shown to increase proportionally with enzyme concentration, further confirming the validity and sensitivity of the colorimetric assay. Additional kinetic data are provided in Figure S-9 of the Supporting Information.

Table 1: Apparent net kinetic parameters for hydrolysis of methyl picolinate by CocE

Analytical Method	No.	[CocE] (μM)	K_M (mM)	V_{max} (pmole/s)	k_{cat} (s^{-1})	k_{cat}/K_M ($M^{-1}s^{-1}$)
HPLC	1	0.148	14.02±6.7	196±20	6.62±0.70	472±50
Spectrophotometry (Plate reader)	2	0.123	16.9±6.0	204±20	8.30±0.70	492±41
	3	0.148	17.3±5.6	234±18	7.89±0.60	456±35
	4	0.177	17.2±5.6	266±20	7.49±0.57	437±33

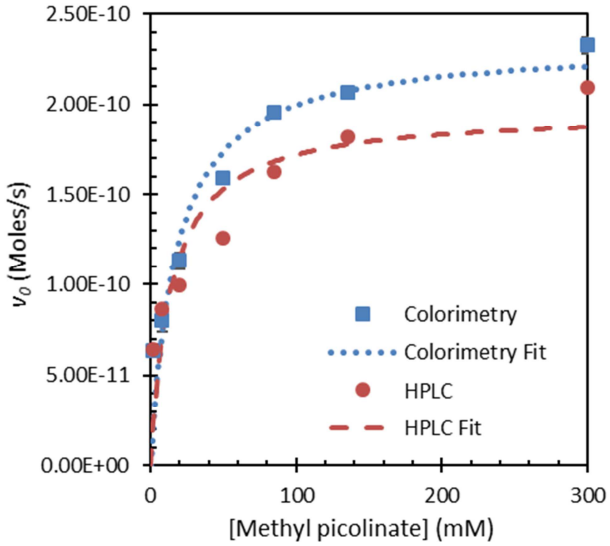

Figure 6: Steady-state kinetics of the hydrolysis of methyl picolinate to picolinate and methanol by wild-type cocaine esterase (CocE) (0.148 μM), as determined by spectrophotometry (blue squares) and by HPLC (red circles). The blue dotted curve and red dashed curve represent the best fit of the spectrophotometry and HPLC data, respectively, to the Michaelis-Menten equation.

The ability of the colorimetric assay to capture kinetic parameters for both the hydrolysis of methyl picolinate by AEH and the hydrolysis of ampicillin by AEH was consistent with the liberation of a carboxylic acid causing solution pH to decrease as either reaction progresses. Both analytical methods evaluated here, HPLC and colorimetry, revealed kinetic data consistent with each other and supported the use of pH-based colorimetry as a viable alternative to HPLC.

3.3 Differentiation Between Synthesis and Hydrolysis Activity

To demonstrate that the colorimetric assay was able to differentiate between synthesis and hydrolysis activity, a model reaction with D-PGME serving as the sole substrate was implemented (Figure 2). Because the colorimetric assay was shown to be sensitive to pH, hydrolysis reactions that decreased the pH value of initially neutral solutions could be distinguished from amide bond forming synthesis reactions that increased the pH value of initially neutral solutions. The hydrolysis and synthesis reactions of 25 mM D-PGME by either CocE or a thermally stabilized variant of wild type AEH (AEH QV-H) were evaluated, and the solution pH was indirectly monitored by tracking the absorbance of phenol red at 557 nm in the reaction mixtures (Figure 7).

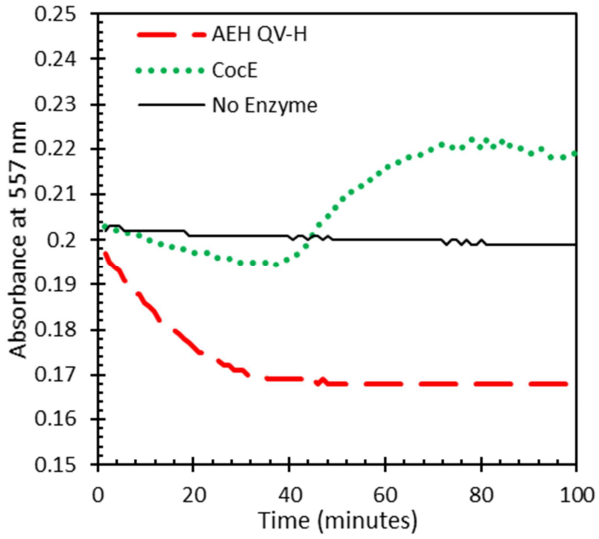

Figure 7: Absorbance at 557 nm over time for reaction mixtures containing 25 mM D-PGME and either AEH QV-H (red) or CocE (green). A control with no enzyme is also shown (black). All reactions occur in 100 mM PO_4, 20 °C, and are initially at pH 7.0.

While all three reaction mixtures began at the same neutral pH value, they each exhibited different behaviors in the colorimetric assay. The non-enzymatic control showed no appreciable change in pH, which was consistent with the lack of any appreciable conversion. Both the AEH- and CocE-catalyzed reactions initially dropped in absorbance. This decrease in the measured absorbance of phenol red was attributed to a decrease in the pH value of the solution, and was consistent with the carboxylic acid production associated with the hydrolysis reactions (Figure 2). In the AEH-catalyzed reaction, this decrease continued unabated until all activity stopped, which was consistent with reports that the QV-H variant used did not exhibit measurable *n*-phenylgycyl polymer synthesis activity (Figure 2).[6] For the CocE-catalyzed reaction, the decrease in absorbance was more gradual, and was eventually overtaken by a greater magnitude increase in absorbance after 45 minutes (Figure 7). These results were consistent with the CocE reaction exhibiting competing pH effects, likely due to the presence of both hydrolysis and synthesis reactions (Figure 2). Although the mechanism behind the initial decrease in pH prior to the increase in pH warrants future investigations, it is likely that the rate of primary hydrolysis initially outpaced synthesis due to uncoupling; as excess D-PGME was eliminated, fewer primary hydrolysis side-reactions occurred leading to more efficient catalysis of *n*-phenylgycyl polymer synthesis from the available D-PGME remaining in solution. Synthesis of dipeptide methyl ester by CocE was confirmed by liquid chromatography mass spectrometry (LCMS) analysis (Figure S-11).

3.4 Prediction of Assay Response Curves

The mathematical model described above and provided in the Supporting Information was used to predict the assay response to hydrolysis of methyl picolinate (Figure 5) under different conditions. Reaction mixtures with concentrations of 20, 50, or 85 mM methyl picolinate in 100 mM sodium phosphate were predicted by modeling and confirmed by experimental measurements of physical samples simulating various conversion levels, prepared by mixing methyl picolinate, picolinic acid, and methanol in predefined ratios as described in the Methods section. The model predictions and experimental measurements of simulated samples are shown in Figure 8.

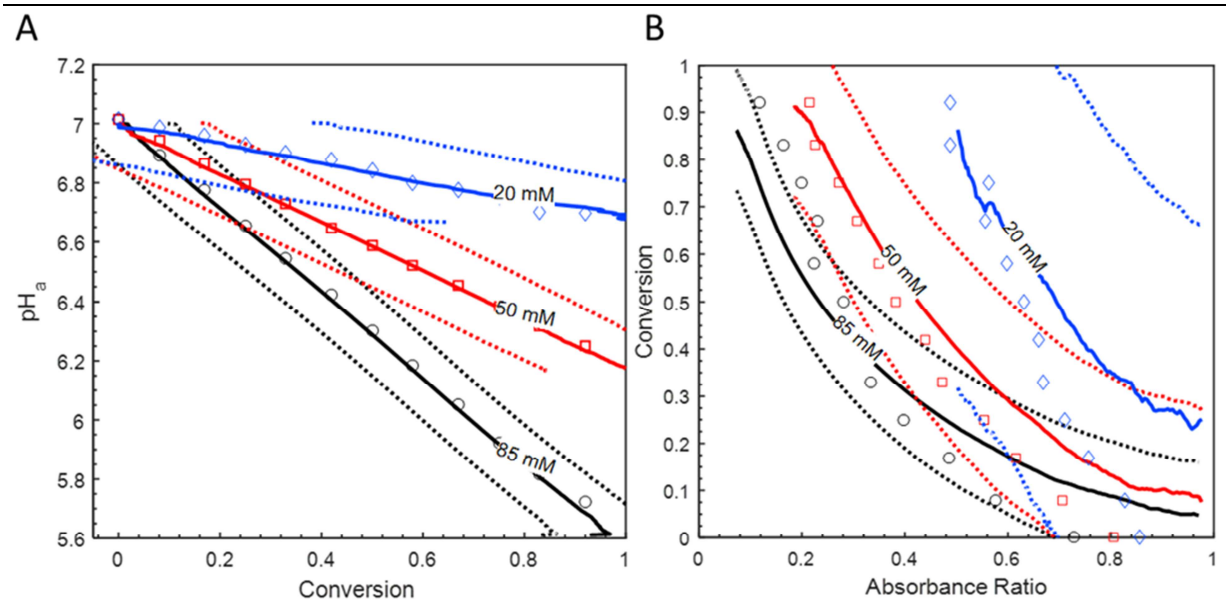

Figure 8: Model predictions and simulated (non-enzymatic) reaction data for the hydrolysis of either 20 mM (blue, diamonds), 50 mM (red, squares), or 85 mM (black, circles) methyl picolinate in 100 mM sodium phosphate buffer. Panel A: pH_a vs. Conversion. This is the expected change in measured pH over the course of each reaction. Panel B: Conversion vs. Absorbance Ratio. This is the expected relationship between the reaction conversion and the measured absorbance ratio (557 nm / 479 nm) of phenol red in the assay. In both panels: simulated experimental data (manually prepared samples designed to different conversion points in the hydrolysis reactions) are plotted as open symbols, and model predictions are plotted as curves. Solid lines show the mean prediction value, while uncertainty estimates at ±1 standard deviation for 10,000 Monte Carlo samples are indicated by the dashed lines.

In all three predictions (i.e., for initial substrate concentrations of 20, 50, and 85 mM), samples initially at neutral pH value begin to acidify as hydrolysis proceeds, and the model predictions match the experimentally measured samples within the estimated prediction error. In general, the magnitude of the pH change is an effect of the background buffer capacity as well as the pK_a values and concentrations of the hydrolysis reactants and products. For a given (nonzero) conversion level, samples prepared with more substrate will have a greater amount of carboxylic acid product, and thus a greater propensity to overcome the pH-stabilizing effect of the phosphate buffer. Both the predictions and experimental data support this reasoning, and it is apparent in Panel A of Figure 8 that the 85 mM curve has the greatest magnitude slope, and 20 mM the least. The range of the assay within the pH-range of the colorimetric indicator (here, phenol red) dictates the shape of the plot of absorbance ratio vs. reaction conversion. As the pH response in Panel A is relatively linear, and the absorbance response of the indicator is sigmoidal (Supporting Information, Figures S-5 and S-6), the absorbance vs. conversion relationship for these samples is distorted and transformed sigmoidal sections. The nonlinear and widely variable nature of the relationship between the observable color change and the reaction progress is the reason that either experimental or simulated standard curves, or the pH equilibrium model described in this work are required to reliably interpret experimental assay results.

The slope of the relationship between pH and conversion is inherently linked to the sensitivity of the assay, with greater magnitude changes in pH corresponding to a more sensitive assay. This result is captured by the width of the uncertainty bands in Panel B of Figure 8, which are widest for the sample with 20 mM substrate, and narrowest for the sample with 85 mM substrate.

3.5 Hypothesis Testing and Interpretation of Assay Results

Two example assay samples were prepared to evaluate whether CocE would be classified as a ‘hit’ or a ‘miss’ in a first-pass high throughput screen (evaluating either enzyme variants or substrate alternatives). Reaction mixes containing phenol red, 50 mM methyl picolinate, and either CocE or a non-enzymatic control in 100 mM sodium phosphate were tracked in a plate reader over several hours. The ratio of optical absorbance (557 nm)/(479 nm) is shown over time in the top panel of Figure 9. The non-enzymatic sample maintains a relatively steady absorbance ratio while the absorbance ratio of the sample containing CocE drops over several hours. Using the model predictions of conversion against absorbance ratio (Figure 8, Panel B) and the supplied spreadsheet for data interpretation and hypothesis testing as described in the Methods section, these absorbance ratios were converted to predictions of conversion with associated levels of prediction uncertainty (Figure 9, middle panel). The results of automatic hypothesis testing, comparing the enzymatic and non-enzymatic samples, are shown in the bottom panel of Figure 9,

and the null hypothesis is rejected after 20 minutes indicating that CocE has a statistically significant influence on reaction conversion, and is therefore a 'hit' in this assay. This result is consistent with the established function of CocE as a catalyst for the hydrolysis of methyl picolinate, and supports the use of pH-based colorimetry with model predictions and hypothesis testing for enzyme or substrate screening.

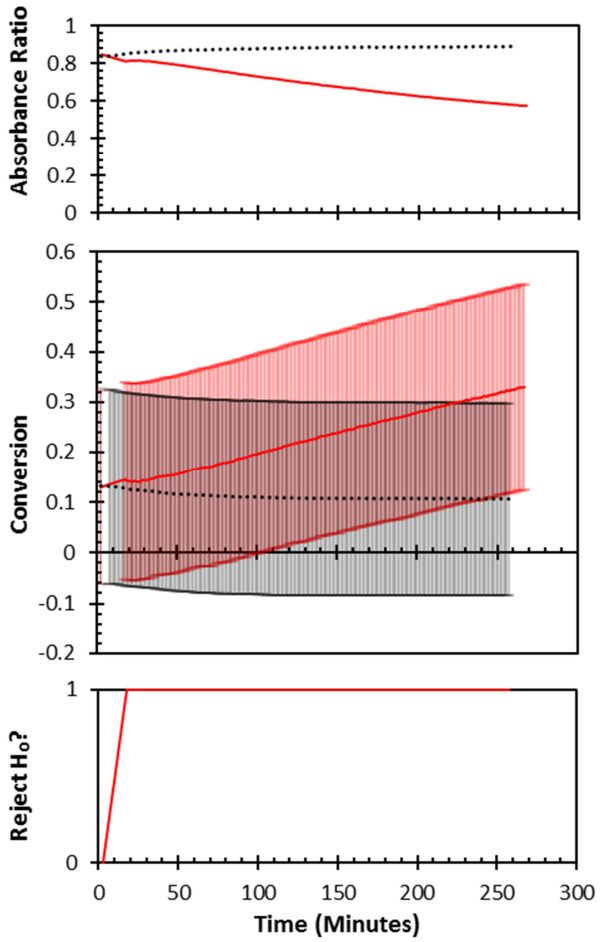

Figure 9: Use of model predictions to perform hypothesis testing. The top panel shows the absorbance ratio (557 nm/479 nm) over time for the hydrolysis of 50 mM methyl picolinate in 100 mM sodium phosphate by CocE (solid red), and non-enzymatic control (dotted black). In the center panel, these data are transformed into hydrolysis conversion, with error bars at ± 1 standard deviation, after Monte Carlo simulation. The bottom panel illustrates how Welch's t-test rejects the null hypothesis within twenty minutes using a p-value threshold of $\alpha = 0.05$.

4 Discussion

4.1 Summary of Results

The experimental results presented provide general support and validation for the application of pH-based colorimetry and modeling to high throughput reaction screening. Several intermediate steps were taken to build up to the use of pH and phenol red to track enzymatic reactions, as well as to model and verify predictions of assay behavior for use in high throughput hypothesis testing. Multiple enzymatic hydrolysis and synthesis reactions, listed in Table 2, were used to validate each of the different parts of this work. Phenol red was demonstrated to predictably reveal – but not interfere with – enzymatic synthesis and hydrolysis reactions (reactions 1 and 2 in Table 2). Colorimetry and HPLC were shown to produce comparable results for kinetic analysis of both CocE and AEH (reactions 2 and 3). Colorimetry was also shown to differentiate between reaction regimes dominated by hydrolysis or synthesis activity (reactions 4 and 5).

Table 2: Hydrolysis and synthesis reactions evaluated in this study.					
No.	**Substrate**	**Enzymes**	**Expected Products**		**Reaction Type**
1	6-aminopenicillinate and D-phenylglycine methyl ester	AEH	ampicillin	methanol	synthesis
2	methyl picolinate	CocE	picolinate	methanol	hydrolysis
3	ampicillin	CocE, AEH	6-aminopenicillinate	D-phenylglycine	hydrolysis
3	D-phenylglycine methyl ester	AEH	D-phenylglycine	methanol	hydrolysis
5	D-phenylglycine methyl ester	CocE	di- and tri-peptides	methanol	synthesis

A generalizable mathematical model was shown to accurately predict the response of the colorimetric assay to experimental samples simulating reaction 2 at various levels of conversion and performed under varied conditions. Finally, an automated hypothesis test correctly classified CocE as having activity on methyl picolinate in an assay trial (reaction 2). These data are the result of a limited range of experiments, but the principles behind them are sufficiently general to warrant further investigation into the combination of pH-based colorimetry and modeling of pH equilibria for high throughput assays and screening tests.

4.2 Limitations of the pH-Based Assay

The framework we present for colorimetric pH-based assays have the potential to accelerate the development of hydrolase enzymes, such as those utilized for the biocatalytic synthesis of β-LA, by enabling efficient high-throughput analysis of enzyme variants, substrates, or reaction conditions. These benefits notwithstanding, there are some general cases in which the assay or mathematical model presented here may not be appropriate. It is inadvisable to use this assay for reactions with unknown side product formation, because the exact hydrolysis stoichiometry, as well as the acidity constants of all ionizable species, is necessary for the prediction of assay response curves. Additionally, the model presented here should not be used for reactions that will exceed ionic strengths of 0.5 M – the recommended limit of Sun's extended Debye-Hückel parameterization.[19] Beyond this range, specific ion interactions may convolute simplified attempts at activity correction, and more detailed models are recommended. Finally, even when all of the above criteria are met, a particular set of assay conditions might not provide satisfactory sensitivity for a particular reaction. In such cases, slight adjustments to experimental conditions – such as reducing the buffer concentration or starting at a different pH value – may resolve these issues.

In general, the experimental results in Figure 7 indicate that this assay approach would be effective for researchers looking to increase either amide synthesis or ester hydrolysis activity by compressing results into simple increases or decreases in absorbance. Nevertheless, there are limitations that must be considered: the assay would not be able to capture equal and simultaneous increases in both activities due to their opposing effects on solution pH, and certain hydrolysis reactions, such as those of amides, produce equimolar amounts of acid and base, significantly adding to the buffering capacity of the reaction system around a certain pH value. If that particular pH value happens to be the same as the initial pH of the assay, then the pH will not change as a function of conversion. Mathematically speaking, the algebraic solutions to the pH equilibrium model become undefined, as the physical system they are modeling adopts a one-to-many mapping from pH to conversion. This effect is illustrated in Figure 10, which shows the predicted pH response to the hydrolysis of 300 mM acetamide. Acetamide hydrolysis produces equimolar acetic acid and ammonia (Figure 11), which are commonly used together to buffer solutions to pH 7.0. Therefore, no matter the starting pH, the solution will tend towards neutrality. Since CocE is most active at neutral pH, the assay must start at pH 7, meaning that the predicted assay response is undefined.

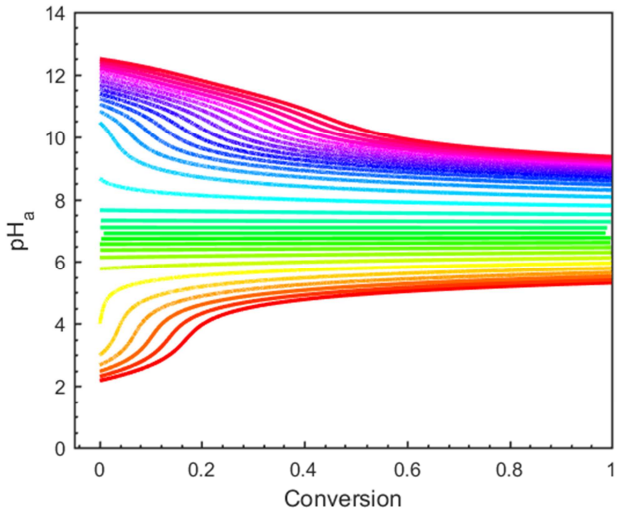

Figure 10: The predicted pH response to conversion for hydrolysis of 300 mM acetamide, over a wide (exaggerated, for emphasis) range of starting pH values. The tendency of the pH value towards neutral illustrates a fundamental limitation of the pH-equilibrium model and colorimetric assay.

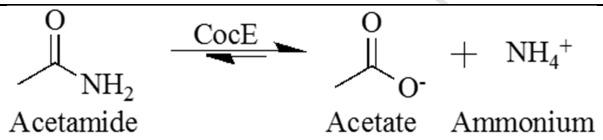

Figure 11: Wild-type CocE can catalyze the hydrolysis of acetamide into acetate and ammonium.

Finally, this approach should only be used for first-pass screening, as the extended Debye-Hückel method used here is an empirical regression of experimental data, and may not provide satisfactory results for all compounds. As with most colorimetric assays, insoluble and precipitating components will hinder correct measurements; assays should be performed within the solubility limits of all reagents.

4.3 Advantages of the pH-Based Assay over Existing Methods

In traditional HPLC-based assays, the elution time and absorbance level of each compound are affected by the pH of the mobile phase, as well as the column condition and temperature. Additionally, chromatography columns rely on dynamic cross-linked functional groups that may exhibit varied behavior under different conditions of mobile phase, storage solvents, upkeep level, and age. These variables are difficult to control, and failure to do so can result in peak-splitting, degradation of assay quality, and inconsistent results. Furthermore, designing separation methods for and producing standard curves for a wide variety of possible reactants and products is time consuming, and may require switching between multiple HPLC columns or mobile phases. Finally, the challenges of using HPLC for high-throughput analysis are exacerbated by the prolonged sample run-time – typically requiring at least 30 minutes to collect a single data point.

As optical measurements in general are simpler and faster than HPLC, switching a first-pass screening operation from HPLC to colorimetry could result in a significant reduction in time and material costs, as well as the volume of data, in comparison to HPLC. Using the phenol red assay, multiple enzymatic reactions can be loaded into a standard well-plate and can be reliably qualified as ‘hit’ or ‘miss’ in 100 minutes or less. Additionally, if hypothesis testing is performed in real-time during absorbance measurement, then a consistently low p-value may permit early termination of a sample. This is illustrated for the hydrolysis of 50 mM methyl picolinate by CocE over several hours in the bottom panel of Figure 9. In this example, it is clear after less than an hour that the hydrolysis of 50 mM methyl picolinate should be considered a positive ‘hit,’ and that the assay (or monitoring of that particular set of samples) may be terminated early. There are also other benefits to continuously monitoring assay samples: a reduced number of samples can be used, as repeated observation of an individual sample provides an effective denoising, and time-series data provide opportunities for other uncertainty-management approaches such as low-pass filters, or more sophisticated statistical methods involving sequential analysis.

Alternative high throughput colorimetric assays exist for these and other reactions, but the current paradigm in which every reaction must have its own specialized assay may not be the most efficient use of resources. The method presented here relies only on acid-base equilibria, and is therefore generalizable to the analysis of many reactions and enzymes. The mathematical model can predict direct mappings between optical absorbance and conversion for a variety of reactions without necessarily requiring experimental standards, and cases in which the colorimetric assay will not work can frequently be determined in advance of any experimentation in the laboratory.

5 Conclusions

The use of phenol red as an indicator for high-throughput pH-based colorimetric substrate scanning and activity screening of enzyme variants was demonstrated to be successful. This assay can be employed to detect reactions catalyzed by AEH and CocE as well as other enzymes within the α/β hydrolase family, and can be used to distinguish hydrolysis from synthesis activity. A thermodynamic pH equilibrium and reaction-conversion model compresses the multitude of variables embodied in a reaction system into simple and direct relationships between optical absorbance and reaction conversion. This model provides insights into assay behavior that facilitate planning of experiments. Model predictions can be used in lieu of experimental standard curves – the collection of which might detract from the otherwise high-throughput nature of the assay – and facilitate real-time hypothesis testing to classify samples as hits or misses. The approach used here is sufficiently general to enable use of colorimetric pH-based assays for rapid screening of other aqueous reactions, which result in pH changes.

6 Supporting Information

Supporting Information is available on the publication website, and contains the following materials:

1. Supporting Information: Additional figures and enzymatic hydrolysis and synthesis data, as well as detailed explanation of the mathematical model and Mathematica and MATLAB codes. (File type: PDF)

2. Mathematical Model: A compressed zip folder containing the files necessary to run and modify the model described in this paper. (File type: ZIP) The contents of the compressed folder are:

    a. License: A copy of the code license. (File type: .txt)

    b. Model_File_1: Mathematica Input File for algebraically solving equations (3-11). (File type: Mathematica .nb file)

    c. Model_File_2: MATLAB code for the full pH equilibrium model. Requires MATLAB version R2016a or later to run. (File type: MATLAB .m file)

    d. Model_File_3: Microsoft Excel spreadsheet parameterizing the model for the hydrolysis of methyl picolinate. (File type: .xlsx)

7 Acknowledgements

The authors would like to thank Dr. Nils Persson for his thoughtful suggestion of incorporating Monte Carlo simulation for uncertainty propagation and sensitivity analysis, as well as Dr. M. Thomas Morgan, for his insights and discussions relating to thermodynamic activity and ionic strength-associated phenomena.

The authors acknowledge financial support from the National Science Foundation (NSF) under contracts IIP-1540017 and IIP-0969003 to the I/UCRC Center for Pharmaceutical Development (CPD).

8 Keywords

pH • Colorimetric • alpha/beta hydrolase • AEH • CocE

9 Abbreviations

6-APA, 6-Aminopenicillanic acid; APANiB, 5-(2-Amino-2-phenylacetamido)-2-nitrobenzoic; β-LA, β-Lactam antibiotics; °C, Degrees Celsius; CocE, Cocaine esterase; D-PG, D-Phenylglycine; D-PGME, D-Phenylglycine

methyl ester; DTNB, 5,5'-Dithiobis-(2-nitrobenzoic acid); HCl, Hydrochloric acid; HPLC, High performance liquid chromatography; kcat, Catalytic turnover number (s-1); KM, Michaelis-Menten constant (mM); pH, Log of the concentration of protons; pHa, pH reported on an activity basis; QV-G, Quadruple variant of AEH (N186D/A275P/V622I/E143G); QV-H, Quadruple variant of AEH (N186D/A275P/V622I/E143H); NaCl, Sodium chloride; SDS, Sodium dodecylsulfate; NaPO4, Sodium phosphate; UV-Vis, Ultraviolet-visible.

10 References

1. Holmquist, M., Alpha/Beta-hydrolase fold enzymes: structures, functions and mechanisms. *Current Protein & Peptide Science* **2000,** *1* (2), 209-235.
2. Blum, J. K.; Bommarius, A. S., Amino ester hydrolase from *Xanthomonas campestris* pv. campestris, ATCC 33913 for enzymatic synthesis of ampicillin. *Journal of Molecular Catalysis B-Enzymatic* **2010,** *67* (1-2), 21-28.
3. Gao, D.; Narasimhan, D. L.; Macdonald, J.; Brim, R.; Ko, M.-C.; Landry, D. W.; Woods, J. H.; Sunahara, R. K.; Zhan, C.-G., Thermostable variants of cocaine esterase for long-time protection against cocaine toxicity. *Molecular Pharmacology* **2009,** *75* (2), 318-323.
4. Rauwerdink, A.; Kazlauskas, R. J., How the same core catalytic machinery catalyzes 17 different reactions: the serine-histidine-aspartate catalytic triad of α/β-hydrolase fold enzymes. *ACS Catalysis* **2015,** *5* (10), 6153-6176.
5. (a) Huang, X.; Gao, D.; Zhan, C. G., Computational design of a thermostable mutant of cocaine esterase via molecular dynamics simulations. *Organic & Biomolecular Chemistry* **2011,** *9* (11), 4138-4143; (b) Brim, R. L.; Noon, K. R.; Collins, G. T.; Stein, A.; Nichols, J.; Narasimhan, D.; Ko, M. C.; Woods, J. H.; Sunahara, R. K., The fate of bacterial cocaine esterase (CocE): an in vivo study of CocE-mediated cocaine hydrolysis, CocE pharmacokinetics, and CocE elimination. *Journal of Pharmacology and Experimental Therapeutics* **2012,** *340* (1), 83-95.
6. Paye, M. F., Biocatalysis of amide and peptide bond synthesis by cocaine esterase and alpha-amino acid ester hydrolase. *Georgia Institute of Technology* **2017**, 1-149.
7. Blum, J. K., Broadening the enyzme-catalyzed synthesis of semi-synthetic antibiotics. *Georgia Institute of Technology* **2011**, 1-197.
8. Janes, L. E.; Löwendahl, A. C.; Kazlauskas, R. J., Quantitative screening of hydrolase libraries using pH indicators: Identifying active and enantioselective hydrolases. *Chemistry – A European Journal* **1998,** *4* (11), 2324-2331.
9. Yi, D.; Devamani, T.; Abdoul-Zabar, J.; Charmantray, F.; Helaine, V.; Hecquet, L.; Fessner, W.-D., A pH-based high-throughput assay for transketolase: fingerprinting of substrate tolerance and quantitative kinetics. *ChemBioChem* **2012,** *13* (15), 2290-2300.
10. Deng, C.; Chen, R. R., A pH-sensitive assay for galactosyltransferase. *Analytical Biochemistry* **2004,** *330* (2), 219-226.
11. Xiao, Y. Z.; Huo, X. D.; Qian, Y.; Zhang, Y.; Chen, G. Q.; Ouyang, P. K.; Lin, Z. L., Engineering of a CPC acylase using a facile pH indicator assay. *Journal of Industrial Microbiology & Biotechnology* **2014,** *41* (11), 1617-1625.
12. Chapman, E.; Wong, C.-H., A pH sensitive colorometric assay for the high-Throughput screening of enzyme inhibitors and substrates: A case study using kinases. *Bioorganic & Medicinal Chemistry* **2002,** *10* (3), 551-555.
13. El-Obeid, H. A.; Gad-Kariem, E. A.; Al-Rashood, K. A.; Al-Khamees, H. A.; El-Shafie, F. S.; Bawazeer, G. A. M., A selective colorimetric method for the determination of penicillins and cephalosporins with α-aminoacyl functions. *Analytical Letters* **1999,** *32* (14), 2809-2823.
14. Pereira, P. C.; Arends, I. W. C. E.; Sheldon, R. A., A green and expedient synthesis of enantiopure diketopiperazines via enzymatic resolution of unnatural amino acids. *Tetrahedron Letters* **2014,** *55* (36), 4991-4993.
15. Cashman, J. R.; Berkman, C. E.; Underiner, G.; Kolly, C. A.; Hunter, A. D., Cocaine benzoyl thioester: synthesis, kinetics of base hydrolysis, and application to the assay of cocaine esterases. *Chemical Research in Toxicology* **1998,** *11* (8), 895-901.
16. Blum, J. K.; Ricketts, M. D.; Bommarius, A. S., Improved thermostability of AEH by combining B-FIT analysis and structure-guided consensus method. *Journal of Biotechnology* **2012,** *160* (3–4), 214-221.
17. Ellis, K. J.; Morrison, J. F., Buffers of constant ionic strength for studying pH-dependent processes. *Methods in Enzymology* **1982,** *87*, 405-26.
18. Gans, P.; O'Sullivan, B., GLEE, a new computer program for glass electrode calibration. *Talanta* **2000,** *51* (1), 33-7.
19. Sun, M. S.; Harriss, D. K.; Magnuson, V. R., Activity Corrections for Ionic Equilibria in Aqueous Solutions. *Canadian Journal of Chemistry* **1980,** *58* (12), 1253-1257.
20. Burgot, J.-L., *Ionic equilibria in analytical chemistry*. Springer Science+Business Media: New York, 2012.
21. Sawilowski, S. S., Fermat, Schubert, Einstein, and Behrens-Fisher: The probable difference between two means when. *Journal of Modern Applied Statistical Methods* **2002,** *1* (2), 461-472.